

## Article

# Development of a Surface Treatment to Achieve Long-Lasting Antimicrobial Properties and Non-Cytotoxicity through Simultaneous Incorporation of Ag and Zn via Two-Step Micro-Arc Oxidation

Yusuke Tsutsumi <sup>1,\*</sup>, Harumi Tsutsumi <sup>2,\*</sup>, Tomoyo Manaka <sup>3</sup>, Peng Chen <sup>2</sup>, Maki Ashida <sup>2</sup>, Hideki Katayama <sup>1</sup> and Takao Hanawa <sup>2,4</sup>

- <sup>1</sup> Research Center for Structural Materials, National Institute for Materials Science (NIMS), 1-2-1 Sengen, Tsukuba 305-0047, Japan
- <sup>2</sup> Institute of Biomaterials and Bioengineering, Tokyo Medical and Dental University (TMDU), 2-3-10 Kanda-Surugadai, Chiyoda, Tokyo 101-0062, Japan
- <sup>3</sup> Graduate School of Medical and Dental Sciences, Tokyo Medical and Dental University (TMDU), 1-5-45 Yushima, Bunkyo, Tokyo 113-8510, Japan
- <sup>4</sup> Center for Advanced Medical Engineering Research and Development, Kobe University, 1-5-1 Minatojiminamimachi, Chuoku, Kobe 650-0047, Japan
- \* Correspondence: tsutsumi.yusuke@nims.go.jp (Y.T.); mish0h0hami@gmail.com (H.T.); Tel.: +81-029-859-2564 (Y.T.); +81-03-5280-8010 (H.T.)

**Abstract:** A customized micro-arc oxidation (MAO) treatment technique was developed to obtain antibacterial properties with no toxicity on Ti surfaces. A two-step MAO treatment was used to fabricate a specimen containing both Ag and Zn in its surface oxide layer, and the optimal incorporation conditions were determined. Surface characterization by EDS was performed followed by the antibacterial properties against *Escherichia coli* (*E. coli*) and *Staphylococcus aureus* (*S. aureus*) and osteogenic cell compatibility evaluations. In addition, metal ion release tests were performed to evaluate the contents of Ag and Zn and the ion release behavior in order to simulate practical usage. MAO-treated specimens prepared using proper concentrations of Ag and Zn (0.5Ag-5Zn: 0.5 mM AgNO<sub>3</sub> and 5.0 mM ZnCl<sub>2</sub>, respectively) exhibited excellent antibacterial properties against *E. coli* and *S. aureus* and no toxicity to MC3T3-E1 in antibacterial and cytotoxic evaluations, respectively. The antibacterial property of 0.5Ag-5Zn against *S. aureus* was sustained even after two months of immersion in physiological saline, simulating the in vivo environment.

**Keywords:** antibacterial properties; *E. coli*; micro-arc oxidation; *S. aureus*; silver; titanium; zinc



**Citation:** Tsutsumi, Y.; Tsutsumi, H.; Manaka, T.; Chen, P.; Ashida, M.; Katayama, H.; Hanawa, T. Development of a Surface Treatment to Achieve Long-Lasting Antimicrobial Properties and Non-Cytotoxicity through Simultaneous Incorporation of Ag and Zn via Two-Step Micro-Arc Oxidation. *Coatings* **2023**, *13*, 627. <https://doi.org/10.3390/coatings13030627>

Academic Editor: Anita Ioana Visan

Received: 31 January 2023

Revised: 5 March 2023

Accepted: 14 March 2023

Published: 16 March 2023



**Copyright:** © 2023 by the authors. Licensee MDPI, Basel, Switzerland. This article is an open access article distributed under the terms and conditions of the Creative Commons Attribution (CC BY) license (<https://creativecommons.org/licenses/by/4.0/>).

## 1. Introduction

For biomaterials used in implant devices, strong and rapid adhesion between the implant surface and the surrounding bone is required to reduce the healing period and achieve immediate loading. Therefore, Ti and its alloys, which have these properties, are widely used [1–5]. However, in recent years, biofilm formation owing to bacterial adhesion and subsequent colonization on the implant surface has become a major cause of failure in orthopedic and dental implant surgeries [6–10]. Once a biofilm is formed and firmly adheres to an implant, bacterial secretion plays a pivotal role as a barrier against the host defense mechanisms, resulting in difficulty in eliminating pathogens during biofilm formation. Furthermore, in serious cases, the only way to prevent subsequent infections and other undesirable biological reactions is to remove the contaminated devices from the patient.

The easiest strategy for preventing biofilm formation on metallic devices is to reduce the surface roughness and inhibit bacterial adhesion through polishing. In particular, the

increase in surface area and the formation of pockets can increase the number of bacteria on the surface [11,12]. However, smoothing by surface polishing is not the optimal approach for dental implants and orthopedic fixators because they are preferred to have a rough surface to ensure tight bone contact, meaning hard-tissue compatibility. The application of antibacterial agents in implants is also effective for preventing biofilm formation. Much research and development have been performed to achieve antimicrobial properties and to reveal their antibiological mechanisms using antibacterial agents without requiring ultraviolet or visible light irradiation. The strong antimicrobial effect of Ag has been recognized from an early stage; these specific metal elements, including Ag, inhibit bacterial growth and activity by releasing their metal ions. In addition to these metallic elements, nanoparticles such as graphene and its oxides have been found to exhibit antimicrobial effects due to not only the physical effect attributed to their morphology but also the specific oxidizing properties [13–21].

In the case of implant devices, coating, immobilization, or the introduction of these antibacterial agents is required for modified surfaces. Therefore, we focused on the development of a technique used to introduce antimicrobial agents into the surface-treated layer by a simple anodizing process on the implant substrate in an aqueous solution. Ag and Zn ions are suitable agents with good antibacterial properties; therefore, their effects on various bacteria have been examined [22–32]. In addition, simple electrochemical coating processes are available by using water-soluble Ag and Zn compounds in the treatment electrolytes. Thus, surface modification should enable the formation of a biofunctional layer containing Ag and Zn with controlled metal ion releases in order to solve problems associated with biofilms on metallic biomaterials.

Micro-arc oxidation (MAO) is one conventional electrochemical surface treatment of wet processes [33–36]. Under a high voltage condition, specific anodic oxidation with microscopic and dynamically localized discharges occurs on the specimen surface, resulting in the formation of porous oxide layers that incorporate elements from the electrolyte with interconnected pores. Therefore, MAO treatment can be used to incorporate the desired elements dissolved in the electrolyte into the resulting oxide layer.

We previously succeeded in incorporating antibacterial elements such as Ag and Zn into the oxide surface layer using MAO treatment [27–30], and it was found that the mechanisms underlying the antibacterial properties differed among antibacterial elements. Ag exhibits good antibacterial properties against a wide variety of bacterial species [37]. However, because the mechanism underlying the antimicrobial properties is based on ion release, the modified surface loses its antibacterial properties when the released Ag ions are depleted, owing to long-term immersion. Thus, it is difficult to maintain antibacterial properties over time with Ag alone. Moreover, because of its high toxicity to cells, even in trace amounts, Ag must be used in minimal concentrations. Some epochal trials have been reported that attempted to control and/or prolong the release of Ag ions [38–44]. These seem to be mostly based on the physical or chemical controlling strategy of an excessive release of Ag ions, especially in the initial stage, by using organic or inorganic materials as supports or combinations. Meanwhile, we considered that the more simplified strategy of covering the challenges of Ag ion release is simple and reasonable by introducing a second element rather than precisely controlling the single ion release of Ag.

In our most recent studies, we focused on the simultaneous incorporation of Ag and Zn via a two-step MAO treatment [45,46]. Zn has been shown to form and accumulate chemical compounds as a result of Zn ion release on its surface, and it exhibits delayed antibacterial properties [47–49]. Ti surface oxides incorporated with Ag and Zn had good antibacterial properties, even after immersion in physiological saline for six months [46]. However, the cytotoxicity has not yet been assessed and must be evaluated to ensure biosafety. Although Zn is less toxic than Ag, the risk of cytotoxicity increases as the amount of Zn introduced into the oxide layer is increased. It is also necessary to investigate whether specific cytotoxicity occurs when Ag and Zn are introduced simultaneously.

Therefore, the objective of this study was to optimize the two-step MAO treatment conditions for Ti surface oxide layers, incorporating both Ag and Zn, with strong and durable antibacterial properties without cytotoxicity. We focused on maximizing the Zn incorporation because excessive Ag incorporation was expected to result in cytotoxicity. Therefore, experiments were performed to determine the critical amount of Zn that can be introduced by the two-step MAO process. The effects of the order of introduction and the amount of Zn on the antibacterial properties and cytotoxicity were investigated. We examined in detail the feasibility of minimizing the amount of Ag incorporated and supplementing the resulting degradation of the antibacterial effect with Zn.

## 2. Materials and Methods

### 2.1. Specimen Preparation

Ag- and Zn-incorporated porous titanium dioxide layers were prepared on commercially pure Ti (Grade 2, Test Materials Co., Ltd., Saitama, Japan) surfaces. Two types of specimen disks with diameters of 8 mm (for the cell compatibility and dissolution tests) and 25 mm (for the EDS measurement and antibacterial test) were fabricated by mechanically cutting Ti rods. The surfaces of the disks were mechanically ground using #150, #320, #600, and #800 grit silicon carbide abrasive papers. After polishing, all of the specimens were washed via ultrasonication in acetone and ethanol for 20 min. The Ti disks were fixed onto polytetrafluoroethylene holders with an O ring. The areas in contact with the electrolyte were 39 mm<sup>2</sup> (7.0 mm in diameter) or 398 mm<sup>2</sup> (22.5 mm in diameter). Further information on the working electrode is provided elsewhere in our previous study [50]. For the counter electrode, a 304 stainless steel plate with a sufficient area ratio to the working electrode was used. The electrolyte used for the MAO treatments was a mixture of 100 mM calcium glycerophosphate and 150 mM calcium acetate, which was defined as the basic composition. Silver nitrate (AgNO<sub>3</sub>) and zinc chloride (ZnCl<sub>2</sub>) were added to the base electrolyte. After filling the electrochemical cell with the electrolyte, the working electrode and the counter electrode were installed and connected to a direct current power supply (PL-650-0.1, Matsusada Precision Inc., Shiga, Japan), and then positive voltage was applied for 10 min at maximum at a constant current density of 251 Am<sup>-2</sup>. The majority of the Ti disks were MAO-treated with an annular untreated area 0.5 mm from the edge. The two-step MAO treatment was conducted as follows. MAO treatment was applied to the first electrolyte until the voltage reached 380 V. The exchange from the first electrolyte to the second electrolyte was performed immediately after the observation of the voltage reaching 380 V. The current was reapplied at an upper limit of 400 V for a total treatment time of 10 min. The specimen prepared using the base electrolyte without Ag or Zn is referred to as "0AgZn". The specimens prepared using a combination of the first and second electrolytes containing  $x$  mM Zn ( $x = 0-7.5$ ) and  $y$  mM Ag ( $y = 0-2.5$ ), respectively, are referred to as " $y$ Zn- $x$ Ag" or " $x$ Ag- $y$ Zn."

### 2.2. Evaluation of Antibacterial Properties

Antibacterial property tests were conducted in accordance with the domestic and international standards JIS Z2801 [51] and ISO 22196:2007 [52], respectively. The proliferation of the anaerobic Gram-negative bacteria *Escherichia coli* (*E. coli*, NBRC3972, NITE, Tokyo, Japan) and anaerobic Gram-positive bacteria *Staphylococcus aureus* (*S. aureus*, NBRC3972, NITE, Tokyo, Japan) was evaluated. A suspension medium was prepared via the 500-fold dilution of a nutrient broth containing 3 gL<sup>-1</sup> meat extract, 10 gL<sup>-1</sup> peptone, and 5 gL<sup>-1</sup> sodium chloride. The pH of the suspension medium was adjusted to between 6.8 and 7.2 using sodium hydroxide and hydrochloric acid. The bacteria were added to the suspension medium to obtain  $3.1 \times 10^6$  colony-forming units (CFUs) per mL. The bacterial suspension (0.1 mL) was then dropped onto the specimen and a cover film was immediately placed. The film-covered specimens were kept in an incubator at 35 °C for 24 h as incubation period. The specimens were then washed with 9.9 mL of the sterile physiological saline. The count

of CFU for viable bacteria suspended in the saline was performed using a medium sheet for *E. coli* (JNC Corp., Tokyo, Japan).

### 2.3. Surface Characterization

Surface characterization was performed on the MAO-treated areas of the specimens. Energy-dispersive X-ray spectroscopy (EDS; S-3400NX, Hitachi High-Technologies Corp., Tokyo, Japan) was used to examine the elemental compositions of the specimens.

### 2.4. Metal Ion Release Evaluation

Metal ion release measurements were performed on the entire specimen. Inductively coupled plasma–mass spectrometry (ICP-MS; ELEMENT XR, Thermo Fisher Scientific, Tokyo, Japan) was used to investigate the amounts of released Ag and Zn ions. The MAO-treated specimens in the electrolyte with and without Ag and Zn under various treatment conditions were incubated in 5 mL of physiological saline (0.9% NaCl). The specimens were then sealed in a polyethylene container to allow for the release of Ag and Zn ions from the specimen surface. Subsequently, they were maintained in a thermostatic chamber at 37 °C with moderate shaking (80–100 rpm). Every seventh day, the pooled solution was transferred as fresh physiological saline. The concentrations of Ag and Zn ions in the tested solutions collected at immersion periods of one week (0–7 days) and two months (48–56 days) were measured using ICP-MS. After the metal ion release of the specimens immersed for different durations was evaluated, the antibacterial properties of the aged specimens were compared to those of the as-prepared specimens.

### 2.5. In Vitro Osteogenic Cell Compatibility Test

MC3T3-E1 cells (RIKEN BioResource Center, Ibaraki, Japan) were maintained in a cell culture medium, which was an alpha modification of Eagle's minimum essential medium ( $\alpha$ -MEM; GIBCO, USA), supplemented with 10% fetal bovine serum (Thermo Fisher Scientific Inc., Waltham, MA, USA), 100 U mL<sup>-1</sup> penicillin, 0.25 mg mL<sup>-1</sup> streptomycin, and 0.25 mg mL<sup>-1</sup> amphotericin B (SIGMA, St. Louis, MO, USA). All specimens were sterilized in 70% ethanol for 20 min and thoroughly rinsed with deionized water and PBS (–) before in vitro testing. The cells were seeded onto sterilized specimens at an approximate initial density of 8000 cells cm<sup>-2</sup>. As a control, cells were seeded onto 0AgZn. All cells were incubated at 37 °C in a humidified atmosphere containing 5% CO<sub>2</sub>. After 72 h of seeding, the Cell Counting Kit-8 assay kit (CCK-8, Dojindo Laboratories, Kumamoto, Japan) was added to each specimen containing cells, and the reaction was continued for 4 h at 37 °C. After incubation, 100  $\mu$ L of reaction solution was transferred to a 96-well microplate. The absorbance of the samples was measured at 450 nm using a microplate reader (Chromate Microplate Reader, Awareness Technology, Palm, FL, USA). The reference wavelength was 630 nm. Tissue culture polystyrene (TCPS) was used as a control specimen to quantify the number of attached cells on each specimen. The cells that were attached to the TCPS were harvested via treatment with trypsin/EDTA, followed by resuspension of the cells in the cell culture medium. The cells in the cell suspension harvested from the TCPS were counted using trypan blue (Trypan Blue Stain 0.4%; Gibco) and a hemocytometer. Standard curves for cell number calibration and light absorbance were generated and used to quantify the number of attached cells on each specimen.

### 2.6. Statistical Analysis

Data obtained from the experiments were calculated from three random specimens. All values are presented as mean  $\pm$  SD, and Student's *t*-test was used for statistical analysis.

## 3. Results and Discussion

### 3.1. Optimization of Ag and Zn Incorporation into Surface Oxide Layer

Figure 1 shows the voltage changes during the single-step MAO treatment with different ZnCl<sub>2</sub> concentrations. When the MAO treatments were performed under 0AgZn

and 2Zn conditions, the voltage continued to increase, and finally reached the maximum value of 400 V. However, the voltage suddenly decreased during treatment in the cases of 5Zn, 7.5Zn, and 10Zn. In these cases, no porous oxide layer was formed on the Ti surface. In our previous study, the same phenomenon was observed when a high concentration of  $\text{AgNO}_3$  was added to the electrolyte [45]. The electrical resistance of the resultant oxide layer was significantly reduced when the concentrations of metal ions in the electrolyte and the introduced metallic species in the oxide layer were too high [47]. Therefore, the growth of the oxide layer, which is a typical phenomenon in valve metals, was inhibited.

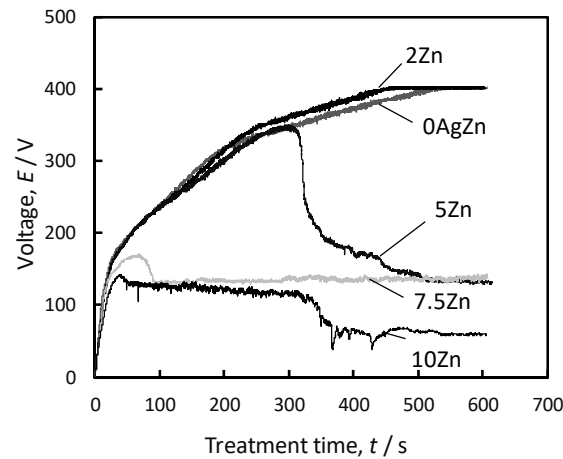


**Figure 1.** Voltage changes during MAO treatment with different  $\text{ZnCl}_2$  concentrations.

Figure 2 shows the voltage changes during the two-step MAO treatment with different  $\text{ZnCl}_2$  concentrations. For 0AgZn-5Zn and 0AgZn-7.5Zn, the treatment was completed without a voltage drop, even though the electrolyte contained a high concentration of Zn ions in the second step. However, when 10mM Zn-containing solution was used, a voltage drop was observed, similar to what occurred in the single-step treatment shown in Figure 1. In contrast to  $\text{AgNO}_3$  [45], the upper limit of the  $\text{ZnCl}_2$  concentration for the two-step MAO treatment was lower than 10 mM; therefore, the optimal  $\text{ZnCl}_2$  concentrations in the electrolyte were determined to be 2 and 5 mM in this study. Finally, a porous oxide layer with a submicron-to-micrometer pore size was successfully formed on the Ti substrate, similar in morphology to the single-step process and previously reported conditions [46,47].

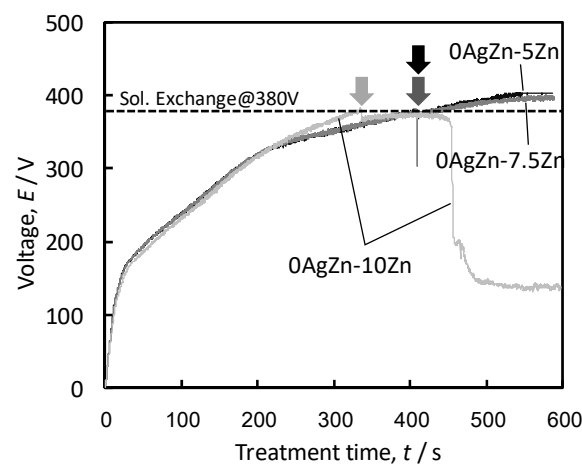


**Figure 2.** Voltage changes during two-step MAO treatment under different second step conditions of Zn concentration. The black and gray arrows indicate when the voltage reached 380 V and the solution was exchanged.

### 3.2. Pre-Evaluation of Antibacterial Property for Screening Treatment Condition

The normalized antibacterial properties of the MAO-treated specimens containing both Ag and Zn were evaluated using *E. coli* (Figure 3). This experiment was performed to establish the MAO treatment conditions for the subsequent experiments described below. In contrast to previous studies [46], electrolytes containing low concentrations of Ag were used as the first treatment solution and 2Zn or 5Zn was used for the second treatment based on the above results. The antibacterial properties of the two-step MAO-treated specimens containing Zn and Ag were improved. In particular, the two-step MAO-treated specimens with low concentrations of Ag exhibited good antibacterial properties when Zn was also introduced appropriately. Initially, Zn was thought to form corrosion products and have only antibacterial properties in a later stage from the implantation; however, it was found that, even in the early stages of the process, when Zn was introduced at high concentrations, it had antibacterial properties. Based on these results, the 0AgZn, 2Zn-0.1Ag, 2Zn-0.5Ag, 0.1Ag-2Zn, 0.5Ag-2Zn, and 0.5Ag-5Zn specimens were investigated in detail to optimize the treatment conditions.

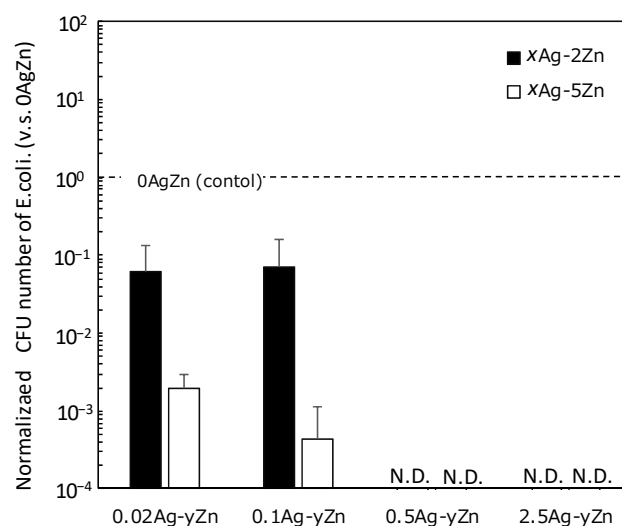


**Figure 3.** Antibacterial properties of MAO-treated specimens containing both Ag and Zn. Measurements were performed on five equally conditioned specimens ( $n = 5$ ). Results in the viable bacterial count  $< 1$  are denoted as “N.D.”.

### 3.3. Characterization of the Specimens Just after the Preparation

The amounts of Ag and Zn incorporated into the surface oxide layer, measured via EDS, are shown in Figure 4a,b, respectively. There were no significant differences in the amount of incorporated Ag, even when the Ag concentration in the electrolyte was increased (2Zn-0.1Ag vs. 2Zn-0.5Ag and 0.1Ag-2Zn vs. 0.5Ag-2Zn) or when the order of treatment using the  $\text{AgNO}_3$ -containing electrolyte was changed (2Zn-0.1Ag vs. 0.1Ag-2Zn and 2Zn-0.5Ag vs. 0.5Ag-2Zn). In the case of the two-step MAO treatment using a highly concentrated  $\text{AgNO}_3$  electrolyte, the amount of Ag incorporated into the surface oxide layer increased as the concentration of  $\text{AgNO}_3$  in the second electrolyte increased as previously reported [45,46]. However, the amount of Ag incorporated in the low-concentration Ag electrolytes was insignificant because the amount of Ag present in the electrolyte was small. In contrast, for Zn, the amount of Zn incorporated into the surface oxide increased as the Zn concentration increased in the two-step MAO treatment electrolyte (0.5Ag-2Zn vs. 0.5Ag-5Zn). However, the order of the solution did not significantly affect the amount of Zn in the surface oxide (2Zn-0.1Ag vs. 0.1Ag-2Zn and 2Zn-0.5Ag vs. 0.5Ag-2Zn). Thus, by using the two-step MAO treatment, a relatively large amount of Zn could be incorporated into the surface oxide layer.

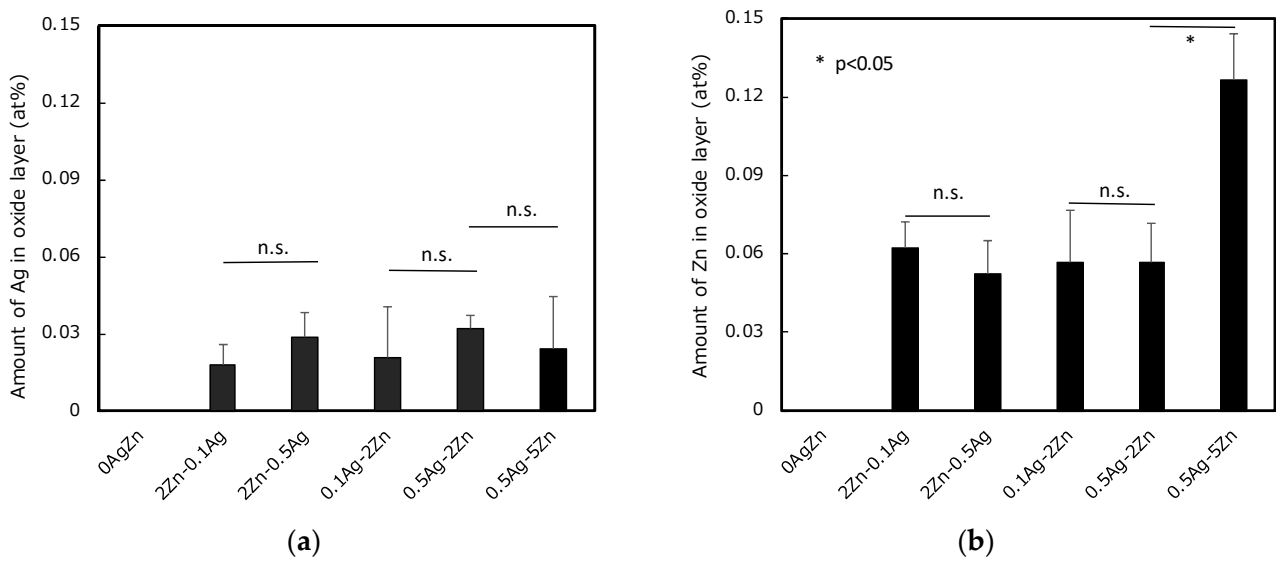


**Figure 4.** Amounts of (a) Ag and (b) Zn in the oxide layer measured via EDS (\* statistically significant difference,  $p < 0.05$ ; n.s.: no significant difference). Measurements were performed on three equally conditioned specimens ( $n = 3$ ).

The antibacterial properties of MAO-treated specimens containing both Ag and Zn against *E. coli* and *S. aureus* after 24 h of culturing are shown in Figure 5a,b, respectively. Almost all of the bacteria survived on the surface of the reference specimens that lacked antibacterial agents (i.e., 0AgZn) against *E. coli* and *S. aureus*. In contrast, all of the specimens subjected to the two-step MAO treatment exhibited strong antibacterial properties, as indicated by the complete absence of *E. coli* and *S. aureus*.

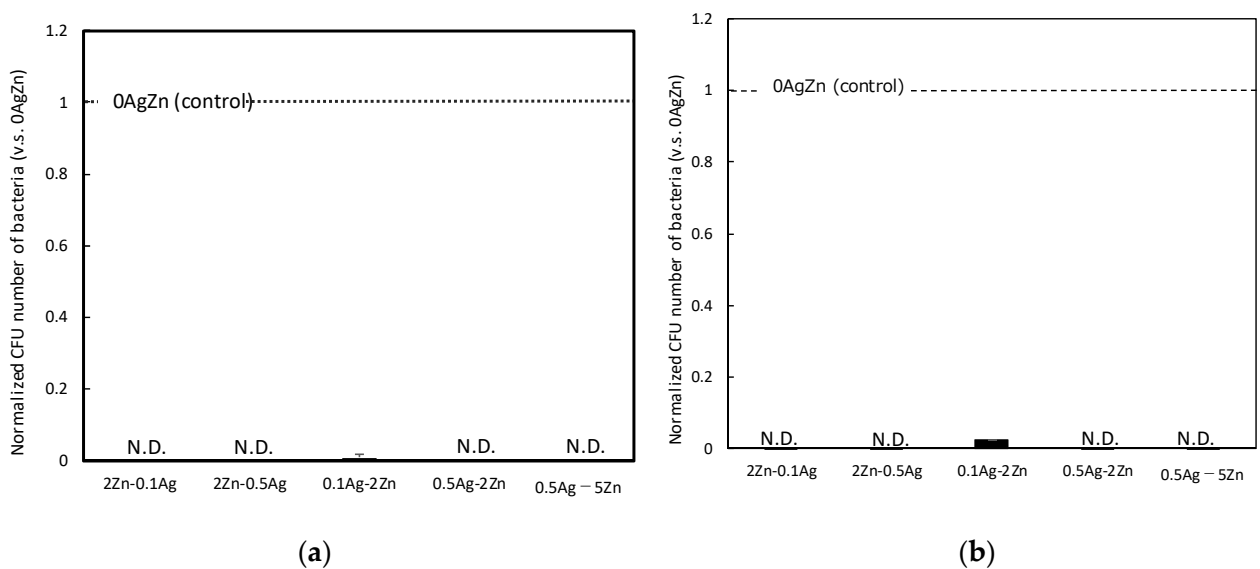


**Figure 5.** Amounts of (a) Ag and (b) Zn in the oxide layer measured via EDS. Measurements were performed on five equally conditioned specimens ( $n = 5$ ). Results in the viable bacterial count  $< 1$  are denoted as “N.D.”.

Figure 6 shows the normalized number of MC3T3-E1 cells on each specimen 72 h after seeding. Although 2.5Ag (positive control) exhibited a significantly smaller number of cells than 0AgZn, the 2Zn-0.1Ag, 0.1Ag-2Zn, 0.5-2Zn, and 0.5Ag-5Zn specimens exhibited a cell viability similar to that of 0AgZn, and a lower cytotoxicity. For 2Zn-0.5Ag, the cell viability decreased significantly compared to the other specimens containing both Ag and Zn. When

the Ag concentration increased (2Zn-0.1Ag vs. 2Zn-0.5Ag), the cell viability decreased because excess Ag ion release resulted in a cytotoxic effect on the osteogenic cells [53–58]. In addition, the cell viability was compared between specimens prepared in the same solution with different orders of introduction (2Zn-0.5Ag vs. 0.5Ag-2Zn). The results indicated that the cell viability decreased significantly when Ag was introduced in the second step (high voltage of 380–400 V). We previously reported that, during MAO treatment, elements in the electrolyte are more easily incorporated at a higher voltage [31]. Although no significant difference in the amount of Ag was observed in the EDS results shown in Figure 4a, the viability of the MC3T3 cells decreased significantly with an increasing Ag concentration in the second step. It is assumed that the distribution of the incorporated Ag differed according to the depth of the oxide layer. The presence of large amounts of Ag in the top surface layer may have been cytotoxic because more Ag ions were released during the early stages of the culturing test. In contrast, Zn did not inhibit cell proliferation, even at high concentrations; thus, Zn was less toxic than Ag. Therefore, the incorporation of Ag using an electrolyte with a moderate Ag ion concentration in the low-potential region (first step of the MAO treatment) combined with the incorporation of Zn using an electrolyte with a high Zn ion concentration in the higher-potential region (second step of the MAO treatment) is ideal for designing a multibiofunctional material surface with both antibacterial properties and tissue compatibility.

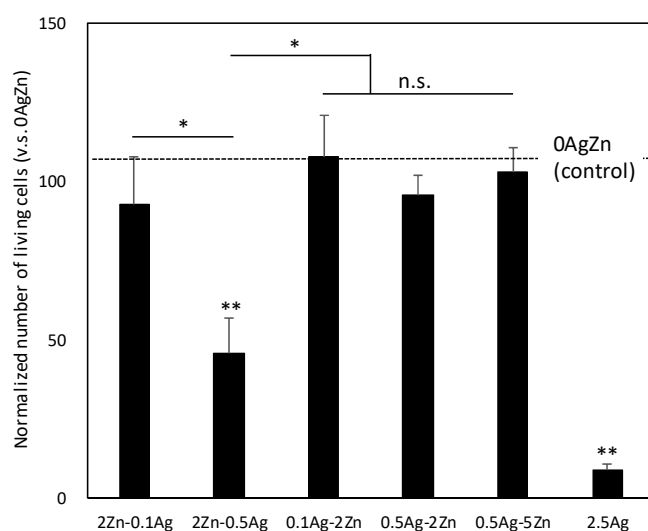


**Figure 6.** Normalized number of living cells on each specimen 72 h after seeding (\* statistically significant difference,  $p < 0.05$ ; n.s.: no significant difference; \*\* statistically significant difference against 0AgZn,  $p < 0.05$ ). Measurements were performed on five equally conditioned specimens ( $n = 5$ ).

### 3.4. Characterization of the Aged Specimens Simulating Long-Term Practical Usage

The durability of the antimicrobial properties was also evaluated in anticipation of the utilization of the proposed treatment for biomedical implants that are placed in vivo and must be maintained for a long period of time (several months after surgery). Figure 7a,b show the amounts of Ag and Zn, respectively, incorporated into the oxide layer after two months of aging (repeated immersion in physiological saline at 310 K) measured via EDS. Compared with the results for the as-prepared specimens shown in Figure 4, the amounts of both Ag and Zn in the oxide film decreased slightly after aging for all specimens. Among the tested specimens, 0.5Ag-5Zn exhibited the highest Zn content.

The amounts of Ag and Zn ions in the physiological saline used for the aging process were measured via ICP-MS. The solution was refreshed with a new one every week. The concentrations of Ag and Zn ions in the first (0–7 d) and eighth (49–56 d) solutions are shown in Figure 8a,b, respectively. For the ICP-MS measurements, a certain level of signal response was detected as the background, even though the solution contained no

elements of interest; For 0AgZn, the calculated values below  $0.1 \mu\text{gL}^{-1}$  were detected as the background. The results obtained by subtracting these backgrounds from the measured raw values can be determined as the amount of Ag and Zn ions released from each specimen. Clearly, more of the elements incorporated in the second-step MAO treatment (high voltage of 380–400 V) in both Ag and Zn ions were released into the solution immediately after aging. This is because the elements were incorporated more efficiently when they were treated at a higher voltage, as described above. Therefore, the number of ions released was higher. After two months of aging, the Ag and Zn contents remained unchanged for 0.1Ag-2Zn, 0.5Ag-2Zn, and 0.5Ag-5Zn, indicating almost no leaching of Ag and Zn. In contrast, 2Zn-0.5Ag continued to release Ag ions after two months of aging, suggesting that the antibacterial properties of 2Zn-0.5Ag may have been maintained after two months of aging (although with a certain level of cytotoxicity). In addition, when Zn was incorporated into the second MAO step (high voltage of 380–400 V), the amount of incorporated Zn increased, and large amounts of Zn ions were released during the initial stage of immersion (0.1Ag-2Zn, 0.5Ag-2Zn, and 0.5Ag-5Zn). After two months of aging, no Zn was released from the specimens (except for 0.5Ag-5Zn), suggesting that the specimens formed corrosion products on the surface oxide [49]. However, relatively large amounts of Zn ions were released from the 0.5Ag-5Zn surface, even after two months of aging, suggesting antibiotic effects, including contact killing owing to the corrosion products [29] and release killing owing to Zn ions.

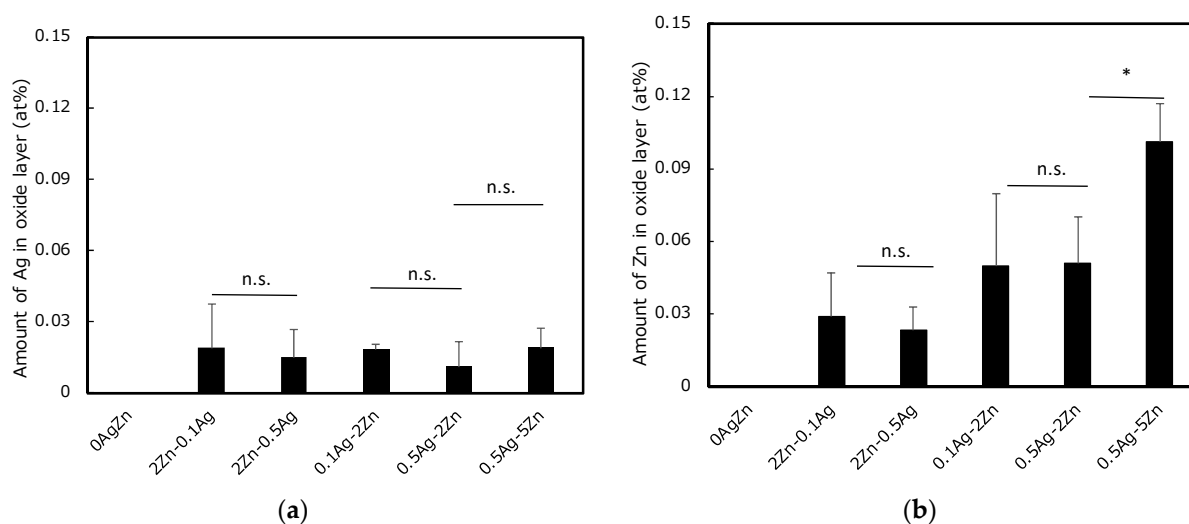


**Figure 7.** Amounts of (a) Ag and (b) Zn in the oxide layer after two months of aging measured via EDS (\* statistically significant difference,  $p < 0.05$ ; n.s.: no significant difference). Measurements were performed on three equally conditioned specimens ( $n = 3$ ).

The antibacterial properties of the MAO-treated specimens containing both Ag and Zn against *E. coli* after two months of aging in physiological saline are shown in Figure 9a. The antibacterial properties of all of the specimens were almost identical to those of 0AgZn. In a previous study [46], a specimen containing Ag and Zn maintained good antibacterial properties for some time, owing to the initial release of Ag ions. It then exhibited a temporary reduction in antibacterial activity after a few months, owing to the depletion of Ag ions. However, after six months, the antibacterial properties improved, owing to the formation of Zn products. Regarding the antibacterial properties against *E. coli*, the two-month aging period used in the present study appeared to be insufficient for achieving antibacterial properties, owing to the accumulation of Zn products. In contrast, the antibacterial property of 0.5Ag-5Zn against *S. aureus* was maintained even after two months of aging. This result indicates that Zn compensates for the reduction in antimicrobial activity, owing to the depletion of Ag ions. In addition, the gradual accumulation of Zn products on the surface oxide layer is expected to enhance the antimicrobial properties, even after two months of

aging. Although this was not confirmed in the present study, it is expected that the degraded antibacterial property against *E. coli* would have been restored after a longer period of testing, as reported in previous studies with six-month testing periods [46]. None of the specimens prepared in the present study were cytotoxic to osteoblast-like cells (Figure 6). MAO-treated specimens are known to promote cellular osteogenesis and exhibit excellent hard-tissue compatibility [49]. The results of this study indicate that long-term antibacterial properties and non-toxicity to osteogenic cells with excellent hard-tissue compatibility can be achieved by optimizing the proposed two-step MAO treatment.

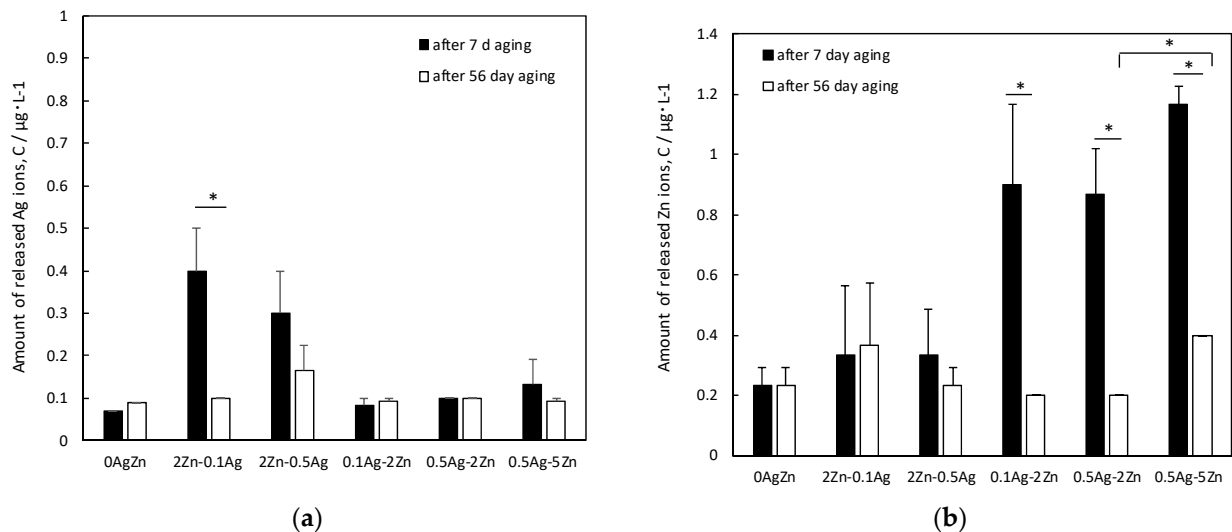


**Figure 8.** Amounts of (a) Ag ions and (b) Zn ions released from the oxide layer into physiological saline (\* statistically significant difference,  $p < 0.05$ ). Measurements were performed on five equally conditioned specimens ( $n = 5$ ).

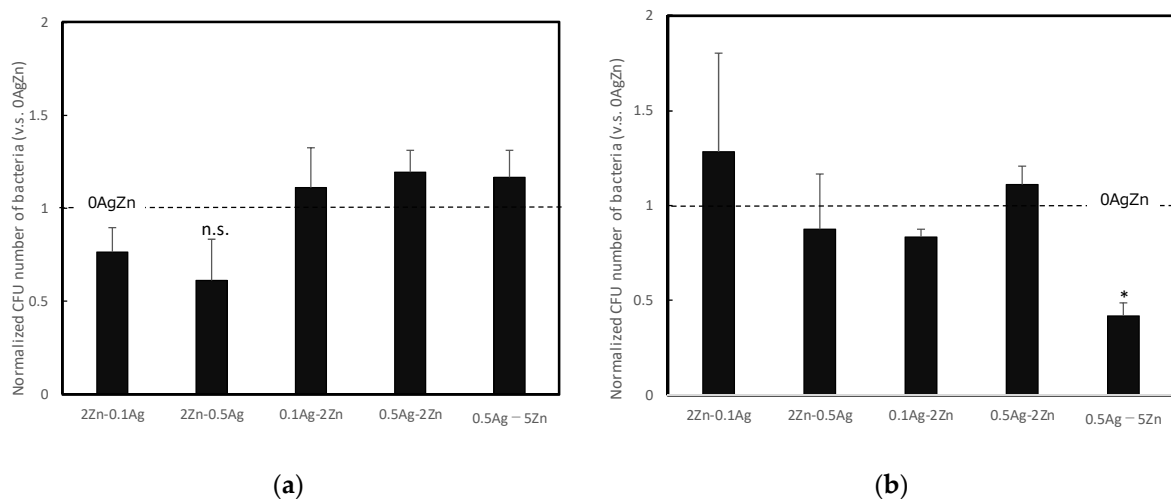


**Figure 9.** Antibacterial properties of MAO-treated specimens containing both Ag and Zn against (a) *E. coli* and (b) *S. aureus* after two months of aging in physiological saline (\* statistically significant difference relative to 0AgZn,  $p < 0.01$ ; n.s.: no significant difference relative to 0AgZn). Measurements were performed on five equally conditioned specimens ( $n = 5$ ).

### 3.5. Limitation and Future Prospective

Finally, it is necessary to mention the limitations and future perspectives of this study. This study revealed that the antibacterial effect can be sustained over a long term due to the complementary effects of Ag and Zn, and that cytotoxicity can be properly avoided

by adjusting the treatment conditions. However, the practical biological environments in which the implant devices will be exposed are extremely complex. In our previous study, it was found that the pore size can be adjusted by the total ionic strength of the electrolyte [59]. The optimization of both structural and compositional parameters of the resulting oxide layer will be inevitable for practical application. This technique is simply based on the metal ion release mechanism; in other words, it is expected to utilize other antimicrobial agents such as graphene nanoparticles, contributing to the innovative development of novel implant surfaces with multiple antimicrobial mechanisms. In this case, additional properties such as the zeta potential would also be subject to optimization for surface treatment conditions to fully utilize the effect of the antimicrobial nanoparticles.

#### 4. Conclusions

Ag and Zn were successfully incorporated onto the Ti surfaces using the proposed two-step MAO treatment, and the surfaces exhibited excellent antibacterial properties against *E. coli* and *S. aureus*. In particular, 0.5Ag-5Zn exhibited sustained antibacterial properties against *S. aureus*, even after two months of aging in physiological saline. The incorporation of Ag and Zn resulted in the release of Ag and Zn ions during the initial stage of aging, which resulted in the formation of Zn products. The release of Ag and Zn ions and the formation of Zn products significantly contributed to the strong and sustained antimicrobial properties in the early and later stages, respectively.

**Author Contributions:** Conceptualization, Y.T., H.T. and T.H.; methodology, Y.T. and T.M.; validation, H.T.; formal analysis, H.T.; investigation, H.T. and T.M.; resources, H.K. and T.H.; data curation, P.C. and M.A.; writing—original draft preparation, Y.T. and H.T.; writing—review and editing, Y.T.; visualization, H.T. and Y.T.; supervision, Y.T.; project administration, Y.T., H.K. and T.H.; funding acquisition, Y.T., H.K. and T.H. All authors have read and agreed to the published version of the manuscript.

**Funding:** This research was partially funded JSPS Research Fellow, grant number JP201940065, and Research Center for Biomedical Engineering (TMDU).

**Institutional Review Board Statement:** Not applicable.

**Informed Consent Statement:** Not applicable.

**Data Availability Statement:** Not applicable.

**Conflicts of Interest:** The authors declare no conflict of interest.

#### References

1. Zubery, Y.; Bichacho, N.; Moses, O.; Tal, H. Immediate loading of modular transitional implants: A histologic and histomorphometric study in dogs. *Int. J. Periodontics Restor. Dent.* **1999**, *19*, 343–353.
2. Hui, E.; Chow, J.; Li, D.; Liu, J.; Wat, P.; Law, H. Immediate provisional for single-tooth implant replacement with Brånemark system: Preliminary report. *Clin. Implant Dent. Relat. Res.* **2001**, *3*, 79–86. [[CrossRef](#)]
3. Cochran, D.L.; Buser, D.; Ten Bruggenkate, C.M.; Weingart, D.; Taylor, T.M.; Bernard, J.P.; Peters, F.; Simpson, J.M. The use of reduced healing times on ITI® implants with a sandblasted and acid-etched (SLA) surface: Early results from clinical trials on ITI® SLA implants. *Clin. Oral Implant. Res.* **2002**, *13*, 144–153. [[CrossRef](#)] [[PubMed](#)]
4. Lorenzoni, M.; Pertl, C.; Zhang, K.; Wimmer, G.; Wegscheider, W.A. Immediate loading of single-tooth implants in the anterior maxilla. Preliminary results after one year. *Clin. Oral Implant. Res.* **2003**, *14*, 180–187. [[CrossRef](#)] [[PubMed](#)]
5. Baltatu, M.S.; Vizureanu, P.; Sandu, A.V.; Florido-Suarez, N.; Saceleanu, M.V.; Mirza-Rosca, J.C. New titanium alloys, promising materials for medical devices. *Materials* **2021**, *14*, 5934. [[CrossRef](#)]
6. Paquette, D.W.; Brodala, N.; Williams, R.C. Risk factors for endosseous dental implant failure. *Dent. Clin. N. Am.* **2006**, *50*, 361–374. [[CrossRef](#)]
7. Dibart, S.; Warbington, M.; Su, M.F.; Skobe, Z. In vitro evaluation of the implant-abutment bacterial seal: The locking taper system. *Int. J. Oral Maxillofac. Implant.* **2005**, *20*, 732–737.
8. Glauser, R.; Schupbach, P.; Gottlow, J.; Hammerle, C.H.F. Periimplant soft tissue barrier at experimental one-piece mini-implants with different surface topography in humans: A light-microscopic overview and histometric analysis. *Clin. Implant. Dent. Relat. Res.* **2005**, *7*, s44–s51. [[CrossRef](#)]

9. Tesmer, M.; Wallet, S.; Koutouzis, T.; Lundgren, T. Bacterial colonization of the dental implant fixture–abutment interface: An in vitro study. *J. Periodontol.* **2009**, *80*, 1991–1997. [[CrossRef](#)]
10. MacKintosh, E.E.; Patel, J.D.; Marchant, R.E.; Anderson, J.M. Effects of biomaterial surface chemistry on the adhesion and biofilm formation of staphylococcus epidermidis in vitro. *J. Biomed. Mater. Res. A* **2006**, *78*, 836–842. [[CrossRef](#)]
11. Ono, M.; Nikaido, T.; Ikeda, M.; Imai, S.; Hanada, N.; Tagami, J.; Matin, K. Surface properties of resin composite materials relative to biofilm formation. *Dent. Mater. J.* **2007**, *26*, 613–622. [[CrossRef](#)] [[PubMed](#)]
12. Meredith, D.O.; Eschbach, L.; Wood, M.A.; Riehle, M.O.; Curtis, A.S.G.; Richards, R.G. Human fibroblast reactions to standard and electropolished titanium and Ti-6Al-7Nb, and electropolished stainless steel. *J. Biomed. Mater. Res. A* **2005**, *75*, 541–555. [[CrossRef](#)] [[PubMed](#)]
13. Akhavan, O.; Ghaderi, E. Toxicity of graphene and graphene oxide nanowalls against bacteria. *ACS Nano* **2010**, *4*, 5731–5736. [[CrossRef](#)] [[PubMed](#)]
14. Dutta, T.; Sarkar, R.; Pakhira, B.; Ghosh, S.; Sarkar, R.; Barui, A.; Sarkar, S. ROS generation by reduced graphene oxide (rGO) induced by visible light showing antibacterial activity: Comparison with graphene oxide (GO). *RSC Adv.* **2005**, *5*, 80192–80195. [[CrossRef](#)]
15. Lakshmi Prasanna, V.; Vijayaraghavan, R. Insight into the Mechanism of Antibacterial Activity of ZnO: Surface Defects Mediated Reactive Oxygen Species even in the Dark. *Langmuir* **2015**, *31*, 9155–9162. [[CrossRef](#)] [[PubMed](#)]
16. Akhavan, O.; Ghaderi, E.; Esfandiari, A. Wrapping bacteria by graphene nanosheets for isolation from environment, reactivation by sonication, and inactivation by near-infrared irradiation. *J. Phys. Chem. B* **2011**, *115*, 6279–6288. [[CrossRef](#)]
17. Liu, S.; Zeng, T.H.; Hofmann, M.; Burcombe, E.; Wei, J.; Jiang, R.; Kong, J.; Chen, Y. Antibacterial activity of graphite, graphite oxide, graphene oxide, and reduced graphene oxide: Membrane and oxidative stress. *ACS Nano* **2011**, *5*, 6971–6980. [[CrossRef](#)]
18. Akhavan, O.; Ghaderi, E. Escherichia coli bacteria reduce graphene oxide to bactericidal graphene in a self-limiting manner. *Carbon* **2012**, *50*, 1853–1860. [[CrossRef](#)]
19. Kumar, A.; Pandey, A.K.; Singh, S.S.; Shanker, R.; Dhawan, A. Engineered ZnO and TiO<sub>2</sub> nanoparticles induce oxidative stress and DNA damage leading to reduced viability of Escherichia coli. *Free. Radic. Biol. Med.* **2011**, *51*, 1872–1881. [[CrossRef](#)]
20. Wang, Y.W.; Cao, A.; Jiang, Y.; Zhang, X.; Liu, J.H.; Liu, Y.; Wang, H. Superior antibacterial activity of zinc oxide/graphene oxide composites originating from high zinc concentration localized around bacteria. *ACS Appl. Mater. Interfaces* **2014**, *6*, 2791–2798. [[CrossRef](#)]
21. Jannesari, M.; Akhavan, O.; Madaah Hosseini, H.R.; Bakhshi, B. Oxygen-Rich Graphene/ZnO<sub>2</sub>-Ag nanoframeworks with pH-Switchable Catalase/Peroxidase activity as O<sub>2</sub> Nanobubble-Self generator for bacterial inactivation. *J. Colloid Interface Sci.* **2023**, *637*, 237–250. [[CrossRef](#)]
22. Koerner, R.J.; Butterworth, L.A.; Mayer, I.V.; Dasbach, R.; Busscher, H.J. Bacterial adhesion to titanium-oxy-nitride (TiNOX) coatings with different resistivities: A novel approach for the development of biomaterials. *Biomaterials* **2002**, *23*, 2835–2840. [[CrossRef](#)] [[PubMed](#)]
23. Simonetti, N.; Simonetti, G.; Bougnol, F.; Scalzo, M. Electrochemical Ag<sup>+</sup> for preservative use. *Appl. Environ. Microbiol.* **1992**, *58*, 3834–3836. [[CrossRef](#)]
24. Wassall, M.A.; Santin, M.; Isalberti, C.; Cannas, M.; Denyer, S.P. Adhesion of bacteria to stainless steel and silver-coated orthopedic external fixation pins. *J. Biomed. Mater. Res.* **1997**, *36*, 325–330. [[CrossRef](#)]
25. Massè, A.; Bruno, A.; Bosetti, M.; Biasibetti, A.; Cannas, M.; Gallinaro, P. Prevention of pin track infection in external fixation with silver coated pins: Clinical and microbiological results. *J. Biomed. Mater. Res.* **2000**, *53*, 600–604. [[CrossRef](#)] [[PubMed](#)]
26. Samani, S.; Hossainipour, S.M.; Tamizifar, M.; Rezaie, H.R. In vitro antibacterial evaluation of sol-gel-derived Zn-, Ag-, and (Zn + Ag)-doped hydroxyapatite coatings against methicillin resistant Staphylococcus aureus. *J. Biomed. Mater. Res. A* **2013**, *101*, 222–230. [[CrossRef](#)] [[PubMed](#)]
27. Jin, G.; Qin, H.; Cao, H.; Qian, S.; Zhao, Y.; Peng, X.; Zhang, X.; Liu, X.; Chu, P.K. Synergistic effects of dual Zn/Ag ion implantation in osteogenic activity and antibacterial ability of titanium. *Biomaterials* **2014**, *35*, 7699–7713. [[CrossRef](#)]
28. Applerot, G.; Lipovsky, A.; Dror, R.; Perkash, N.; Nitzan, Y.; Lubart, R.; Gedanken, A. Enhanced antibacterial activity of nanocrystalline ZnO due to increased ROS-mediated cell injury. *Adv. Funct. Mater.* **2009**, *19*, 842–852. [[CrossRef](#)]
29. Storrer, H.; Stupp, S.I. Cellular response to zinc-containing organoapatite: An in vitro study of proliferation, alkaline phosphatase activity and biomineralization. *Biomaterials* **2005**, *26*, 5492–5499. [[CrossRef](#)]
30. Jones, N.; Ray, B.; Ranjit, K.T.; Manna, A.C. Antibacterial activity of ZnO nanoparticle suspensions on a broad spectrum of microorganisms. *FEMS Microbiol. Lett.* **2008**, *279*, 71–76. [[CrossRef](#)]
31. Dastjerdi, D.; Montazer, M. A review on the application of inorganic nano-structured materials in the modification of textiles: Focus on anti-microbial properties. *Colloids Surf. B* **2010**, *79*, 5–18. [[CrossRef](#)] [[PubMed](#)]
32. Raghupathi, K.R.; Koodali, R.T.; Manna, A.C. Size-dependent bacterial growth inhibition and mechanism of antibacterial activity of zinc oxide nanoparticles. *Langmuir* **2011**, *27*, 4020–4028. [[CrossRef](#)] [[PubMed](#)]
33. Suh, J.Y.; Jang, B.C.; Zhu, X.; Ong, J.L.; Kim, K. Effect of hydrothermally treated anodic oxide films on osteoblast attachment and proliferation. *Biomaterials* **2003**, *24*, 347–355. [[CrossRef](#)] [[PubMed](#)]
34. Son, W.W.; Zhu, X.; Shin, H.I.; Ong, J.L.; Kim, K.H. In vivo histological response to anodized and anodized/hydrothermally treated titanium implants. *J. Biomed. Mater. Res. B Appl. Biomater.* **2003**, *66*, 520–525. [[CrossRef](#)]

35. Kim, D.Y.; Kim, M.; Kim, H.E.; Koh, Y.H.; Kim, H.W.; Jang, J.H. Formation of hydroxyapatite within porous TiO<sub>2</sub> layer by micro-arc oxidation coupled with electrophoretic deposition. *Acta Biomater.* **2009**, *5*, 2196–2205. [CrossRef]
36. Li, Y.; Lee, I.S.; Cui, F.Z.; Choi, S.H. The biocompatibility of nanostructured calcium phosphate coated on micro-arc oxidized titanium. *Biomaterials* **2008**, *29*, 2025–2032. [CrossRef]
37. Rabiee, N.; Ahmadi, S.; Akhavan, O.; Luque, R. Silver and Gold Nanoparticles for Antimicrobial Purposes against Multi-Drug Resistance Bacteria. *Materials* **2022**, *15*, 1799. [CrossRef]
38. Jiang, Y.; Huang, J.; Wu, X.; Ren, Y.; Li, Z.; Ren, J. Controlled release of silver ions from AgNPs using a hydrogel based on konjac glucomannan and chitosan for infected wounds. *Int. J. Biol. Macromol.* **2020**, *149*, 148–157. [CrossRef]
39. Akhavan, O.; Abdolhad, M.; Asadi, R. Storage of Ag nanoparticles in pore-arrays of SU-8 matrix for antibacterial applications. *J. Phys. D Applied Physics* **2009**, *42*, 135416. [CrossRef]
40. Wei, X.; Cai, J.; Lin, S.; Li, F.; Tian, F. Controlled release of monodisperse silver nanoparticles via in situ cross-linked polyvinyl alcohol as benign and antibacterial electrospun nanofibers. *Colloids Surf. B Biointerfaces* **2021**, *197*, 111370. [CrossRef]
41. Akhavan, O.; Abdolhad, M.; Abdi, Y.; Mohajerzadeh, S. Silver nanoparticles within vertically aligned multi-wall carbon nanotubes with open tips for antibacterial purposes. *J. Mater. Chem.* **2010**, *21*, 387–393. [CrossRef]
42. Akhavan, O.; Ghaderi, E. Self-accumulated Ag nanoparticles on mesoporous TiO<sub>2</sub> thin film with high bactericidal activities. *Surf. Coat. Technol.* **2010**, *204*, 3676–3683. [CrossRef]
43. Li, J.; Kang, L.; Wang, B.; Chen, K.; Tian, X.L.; Ge, Z.; Zeng, J.; Xu, J.; Gao, W. Controlled Release and Long-Term Antibacterial Activity of Dialdehyde Nanofibrillated Cellulose/Silver Nanoparticle Composites. *ACS Sustain. Chem. Eng.* **2019**, *7*, 1146–1158. [CrossRef]
44. Akhavan, O.; Ghaderi, E. Capping antibacterial Ag nanorods aligned on Ti interlayer by mesoporous TiO<sub>2</sub> layer. *Surf. Coat. Technol.* **2009**, *203*, 3123–3128. [CrossRef]
45. Shimabukuro, M.; Tsutsumi, H.; Tsutsumi, Y.; Manaka, T.; Chen, P.; Ashida, M.; Ishikawa, K.; Katayama, H.; Hanawa, T. Enhancement of antibacterial property of titanium by two-step micro arc oxidation treatment. *Dent. Mater. J.* **2021**, *40*, 592–598. [CrossRef] [PubMed]
46. Tsutsumi, H.; Tsutsumi, Y.; Shimabukuro, M.; Manaka, T.; Chen, P.; Ashida, M.; Ishikawa, K.; Katayama, H.; Hanawa, T. Investigation of the long-term antibacterial properties of titanium by two-step micro-arc oxidation treatment. *Coatings* **2021**, *11*, 798. [CrossRef]
47. Shimabukuro, M.; Tsutsumi, Y.; Yamada, R.; Ashida, M.; Chen, P.; Doi, H.; Nozaki, K.; Nagai, A.; Hanawa, T. Investigation of realizing both antibacterial property and osteogenic cell compatibility on titanium surface by simple electrochemical treatment. *ACS Biomater. Sci. Eng.* **2019**, *5*, 5623–5630. [CrossRef]
48. Shimabukuro, M. Antibacterial property and biocompatibility of silver, copper, and zinc in titanium dioxide layers incorporated by one-step micro-arc oxidation: A review. *Antibiotics* **2020**, *9*, 716. [CrossRef]
49. Shimabukuro, M.; Tsutsumi, Y.; Nozaki, K.; Chen, P.; Yamada, R.; Ashida, M.; Doi, H.; Nagai, A.; Hanawa, T. Chemical and biological roles of zinc in a porous titanium dioxide layer formed by micro-arc oxidation. *Coatings* **2019**, *9*, 705. [CrossRef]
50. Tanaka, Y.; Kobayashi, E.; Hiromoto, S.; Asami, K.; Imai, H.; Hanawa, T. Calcium phosphate formation on titanium by low voltage electrolytic treatments. *J. Mater. Sci. Mater. Med.* **2007**, *18*, 797–806. [CrossRef]
51. *IS Z 2801:2012; Antimicrobial Products—Test for Antimicrobial Activity and Efficacy*. Japanese Standards Association: Tokyo, Japan, 2012. Available online: <https://www.jisc.go.jp/eng/index.html> (accessed on 30 June 2021).
52. *ISO 22196:2011; Plastics—Measurement of Antibacterial Activity on Plastics Surfaces*. International Organization of Standardization: Geneva, Switzerland, 2011. Available online: <https://www.iso.org/standard/54431.html> (accessed on 30 June 2021).
53. Odnevall Wallinder, I.; Leygraf, C. A critical review on corrosion and runoff from zinc and zinc-based alloys in atmospheric environments. *Corrosion* **2017**, *73*, 1016–1077. [CrossRef] [PubMed]
54. Poon, V.K.M.; Burd, A. In vitro cytotoxicity of silver: Implication for clinical wound care. *Burns* **2004**, *30*, 140–147. [CrossRef] [PubMed]
55. Wataha, J.C.; Lockwood, P.E.; Schedle, A. Effect of silver, copper, mercury, and nickel ions on cellular proliferation during extended, low-dose exposures. *J. Biomed. Mater. Res.* **2000**, *52*, 360–364. [CrossRef] [PubMed]
56. Yamamoto, A.; Honma, R.; Sumita, M. Cytotoxicity evaluation of 43 metal salts using murine fibroblasts and osteoblastic cells. *J. Biomed. Mater. Res.* **1998**, *39*, 331–340. [CrossRef]
57. AshaRani, P.V.; Mun, G.L.K.; Hande, M.P.; Valiyaveetil, S. Cytotoxicity and genotoxicity of silver nanoparticles in human cells. *ACS Nano* **2009**, *3*, 279–290. [CrossRef]
58. Rosário, F.; Hoet, P.; Santos, C.; Oliveira, H. Death and cell cycle progression are differently conditioned by the AgNP size in osteoblast-like cells. *Toxicology* **2016**, *368–369*, 103–115. [CrossRef]
59. Nyan, M.; Tsutsumi, Y.; Oya, K.; Doi, H.; Nomura, N.; Kasugai, S.; Hanawa, T. Synthesis of novel oxide layers on titanium by combination of sputter deposition and micro-arc oxidation techniques. *Dent. Mater. J.* **2011**, *30*, 754–761. [CrossRef]

**Disclaimer/Publisher’s Note:** The statements, opinions and data contained in all publications are solely those of the individual author(s) and contributor(s) and not of MDPI and/or the editor(s). MDPI and/or the editor(s) disclaim responsibility for any injury to people or property resulting from any ideas, methods, instructions or products referred to in the content.